

Realization of Stretch-legged Walking of the Humanoid Robot

Min-Su Kim¹, Inhyeok Kim¹, Sangsin Park¹, Jun Ho Oh¹

¹ HUBO Laboratory, Humanoid Robot Research Center, Department of Mechanical Engineering,

KAIST (Korea Advanced Institute of Science and Technology)

373-1 Guseong-dong Yuseong-gu, Daejon 305-701, South Korea

becool@kaist.ac.kr, inhyeok@kaist.ac.kr, momumima@kaist.ac.kr, jhoh@kaist.ac.kr

Abstract— This paper presents a new forward walking pattern known as stretch-legged walking and posture control algorithm in single support phase. Additionally, what has been termed the Walking Guide Platform (WGP) was developed to verify the developed walking pattern. Walking pattern is generated by simple function such as sine function and 3rd polynomial. Especially pelvis center is generated by 3rd polynomial that is tuned by hip shape factor. The value is selected by experiment. Posture control that is composed of body balancing controller and vibration-reduction controller maintains posture of robot in single support phase. It prevent robot falling in walking. Based on proposed walking pattern, posture control makes realization of stretch-legged walking in humanoid robot.

I. INTRODUCTION

Numerous humanoid biped walking robots such as ASIMO, HRP, HUBO have a viable walking motion [1][2][3][4]. However, these humanoid robots walk while bending their knee. Walking with a bending knee is feasible in the solving of inverse kinematics, and it maintains stability by lowering the center of gravity. It concentrates the load in the knee actuator, and it is hard to realize fast walking. Given that this type of walking is not human-like walking, a human-like walking algorithm was developed recently.

Passive walking proposed by Tad McGeer is representative [5]. Passive walking can walk using its own weight, but it has not been adopted in humanoid biped walking robot that has a hip, knee and ankle joint. Yu Ogura, realized stretch-legged walking using WABIAN-2 [6]. However, this was implemented by the addition of an extra DOF in the waist. Moreover, the waist of this system continues to sway somewhat. E. R. Westervelt showed good forward walking via an analysis of the dynamic walking [7]. However the robot in his study is different from other humanoid robot in that it has no ankle joint. Ankle joints are important in walking, as they play the role of maintaining contact with the ground.

The investigation referred to above are related to human-like walking. Their common feature is stretch-legged walking. Human-like walking uses less energy than walking with a bending knee.

This paper shows the design of a new walking pattern that has a robot walk without bending its knee, and design of a posture control to stabilize the robot in single support phase. In addition, what has been termed the Walking Guide

Platform(WGP) was developed to implement the proposed walking pattern. The Hip Shape Factor(HSF) [4] is introduced to aid with stable walking. The properties are related to the walking speed. Finally, the energy consumption related to walking while bending the knee and walking via proposed walking pattern is compared. Stretch-legged walking in a humanoid robot with a hip, knee, and ankle joint is realized using a simple walking pattern and simple factors, and is shown to be viable in terms of energy consumption.

After verification of proposed walking pattern, stabilization algorithm needs to apply the pattern in humanoid robot. In order to realize stretch-legged walking in humanoid robot, posture control that is composed of body balancing controller and vibration-reduction controller is suggested. The controller is maintain posture of body using ankle joint and IMU(Imperial Measurement Unit). Finally, stretch-legged walking in humanoid robot was realized based on proposed walking pattern and posture control.

II. STRETCH-LEGGED WALKING PATTERN

The typical walking pattern was designed based on a bended knee configuration. The bended knee configuration is unavoidable to maintain the height of the hip. Walking while bending knee has several advantages including lowering the center of gravity and decreasing the landing impact, but it differs from human walking. A human walks and does not bend the knee. A robot cannot walk and maintain its height when its leg is stretched. In order to solve this problem, inverse kinematics is divided into sagittal plane and coronal plane.

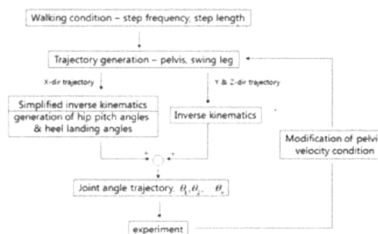


Fig. 1. Process of the generation of the walking pattern generation

A. Trajectory of pelvis center and swing leg.

Cycloid function is used to generate a trajectory of swing leg. As it has zero velocity in initial and final condition and maximum velocity in swing phase, cycloid function is proper.

$$\tilde{x}_A(t) = (b+f)\left(t - \frac{1}{2\pi} \sin(2\pi t)\right) - b \quad (1)$$

The hip trajectory is generated by the 3rd polynomial function. Equation (2)~(4) show the hip trajectory generation process.

$$\tilde{x}_P(t) = \sum_{i=0}^3 a_i \left(\frac{t-t_1}{t_2-t_1} \right)^i \quad (2)$$

$$\begin{bmatrix} 0 & 0 & 0 & 1 \\ 0 & 0 & 1 & 0 \\ 1 & 1 & 1 & 1 \\ 3 & 2 & 1 & 0 \end{bmatrix} \begin{bmatrix} a_3 \\ a_2 \\ a_1 \\ a_0 \end{bmatrix} = \begin{bmatrix} \tilde{x}_P(0) \\ \dot{\tilde{x}}_P(0) \\ \tilde{x}_P(1) \\ \dot{\tilde{x}}_P(1) \end{bmatrix} \quad (3)$$

$$\begin{bmatrix} \tilde{x}_P(0) \\ \dot{\tilde{x}}_P(0) \\ \tilde{x}_P(1) \\ \dot{\tilde{x}}_P(1) \end{bmatrix} = \begin{bmatrix} -b/2 \\ \alpha b \\ f/2 \\ \alpha f \end{bmatrix} \quad (4)$$

Given that the initial position and final position were previously decided, α (hip shape factor) is the only parameter that can be utilized to change the hip trajectory. Fig. 7 shows the various hip trajectories according to the HSF.

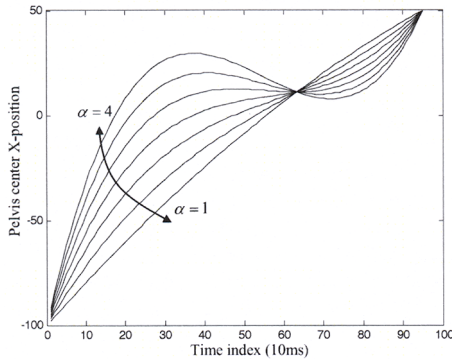


Fig. 2 Hip trajectories according to the HSF

As α increases, initial velocity increases. If α is too large, the hip velocity can be negative. If α is close to 1, the hip trajectory has a nearly constant velocity.

When the walking speed is slow, the robot has insufficient momentum. Thus, a high α can supply sufficient momentum to move the robot forward. However, a small α is adequate when the walking speed is fast; because it has sufficient momentum, extra momentum causes undesired situations.

B. Hip pitch angle and heel landing angle.

Fig. 3 shows the x-dir positions of pelvis center and both feet. For simplicity, the knee is considered fully stretched.

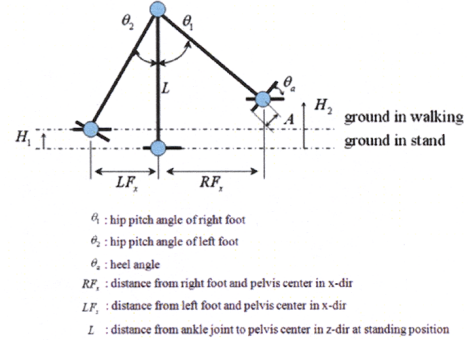


Fig. 3 Hip pitch angle and heel angle related to pelvis and foot position

The hip pitch angles, θ_1, θ_2 were simply calculated using arc-sine function. In addition, the z-dir position of the feet was decided; it was not necessary to consider the z-dir position of the hip

$$\theta_1 = \sin^{-1}\left(\frac{RF_x}{L}\right) \quad (5)$$

$$\theta_2 = \sin^{-1}\left(\frac{LF_x}{L}\right) \quad (6)$$

The above walking pattern has a disadvantage; the landing impact is big. A big impact occurs when the swing leg lands on the ground. When it does this, it brings about unstable walking. To reduce the landing impact, heel landing angle θ_a is applied in the ankle of the swing leg. θ_a plays the role of decreasing the height difference between the swing leg and the support leg; it has the effect of decreasing the landing impact.

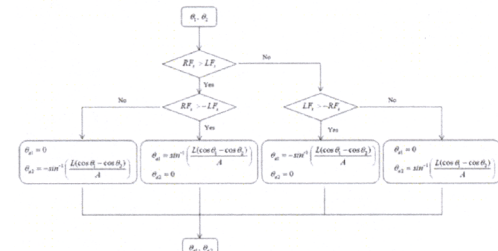


Fig. 4 Process of generating heel landing angle

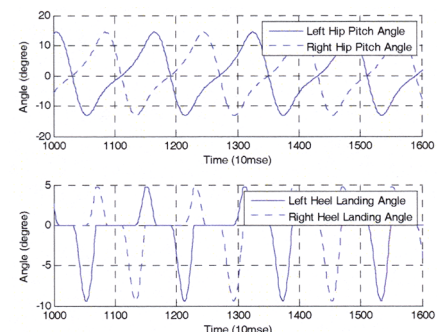


Fig. 5 Hip pitch and heel landing angles

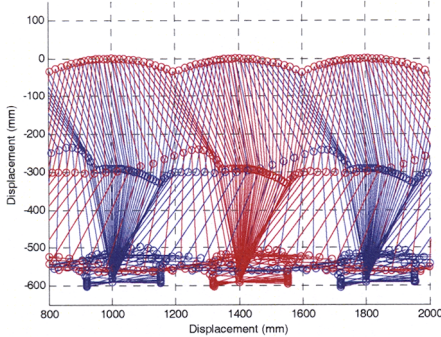


Fig. 6 stretch-legged walking pattern

III. PATTERN VERIFICATION IN SAGITTAL PLANE.

A. Walking guide platform

Walking Guide Platform (WGP) consists of a biped walking robot, a guide system and a treadmill. It constrained the biped walking robot to move in a sagittal plane. The Biped robot has hip pitch, knee pitch and ankle pitch joints in each leg. Therefore, robot can move only in the sagittal plane. Linear motion shafts and a linear bush can help to constrain motions apart from the sagittal plane. A treadmill that operates according to the velocity of the robot was utilized. It helps the robot to walk continuously in a limited space. Fig. 9 shows the DOF of the new biped robot, and TABLE I show the specifications of the actuators.

TABLE I
Specification of the actuators

Joint	Motor	HarmonicDrive
Hip pitch	150W *2	120:1
Knee pitch	150W *2	160:1
Ankle pitch	90W	120:1

Fig. 7 shows the biped robot and the guide system supporting the robot. It has a 2000mm stroke in the x-dir and a 400mm stroke in the z-dir, and is sufficient for the experiments involving the forward walking of the robot. An LM shaft and a linear bushing were used to support the biped robot. As general walking involve numerous disturbances, it is difficult to develop various forward walking patterns. The guide system is a good solution. It can block disturbances from other motions apart from the sagittal plane. This allows the conducting of various experiments in forward walking.

The treadmill allows the robot to achieve infinite walking in a limited space. It rotates automatically according to velocity of the robot, which allows limited attention toward the operation of the treadmill. Fig. 8 shows the treadmill and the devices for velocity control.

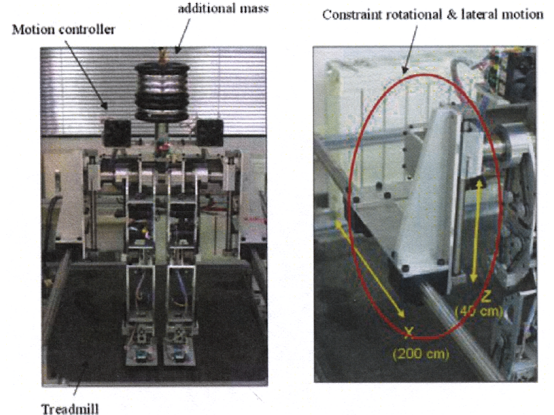


Fig. 7 Biped robot and guide system.

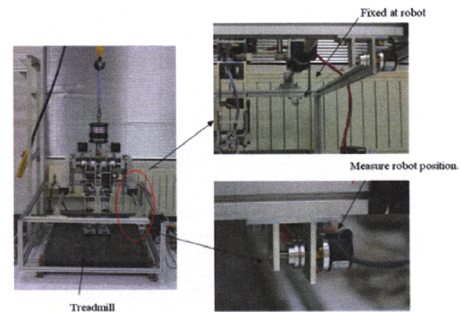


Fig. 8 Treadmill and device for velocity control

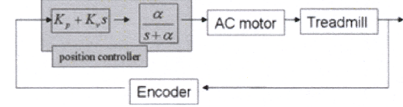


Fig. 9 Control structure of treadmill

The robot and the treadmill are connected using wire and spring, and the relative displacement was measured using an incremental encoder. Fig. 9 shows the control structure of the treadmill. A simple PD-controller and low-pass filter were used to control treadmill. TMSF2403 was used to implement this. The low-pass filter serves to minimize drastic velocity changes. If the robot does not maintain uniform velocity, the treadmill offsets this condition by changing its velocity. As the change of velocity affects the walking of the robot, a low-pass filter was used.

B. Experiment.

To measure the index of walking, the x-dir ZMP and the body tilt angle θ_p were used. Fig. 10 shows the two index parameters.

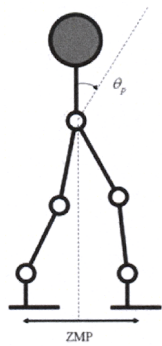


Fig. 10 Index parameter for walking.

When the robot walks stably, ZMP and θ_p maintain a constant values. However, under unstable condition, these index values fluctuate greatly. The deviations of index values are important in stable walking. We judged a stable walking by deviation of index. In order to select best α , walking experiments were done about several α values.

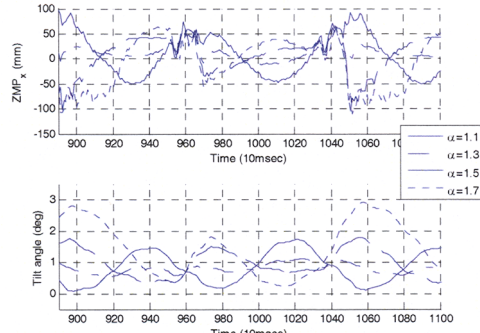


Fig. 11 Step length: 200mm.

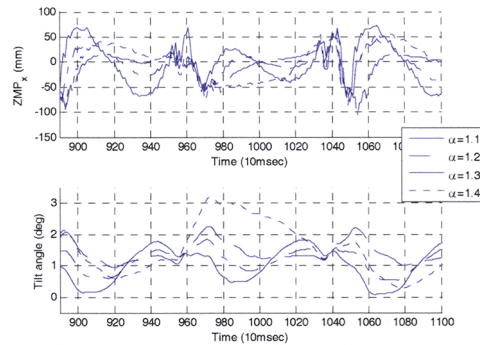


Fig. 12 Step length: 300mm.

Figs. 11, 12 show that the ZMP and θ_p values can change according to the α . For a 200mm step length, the best result occurs when α ranges from 1.3 to 1.4, but the best result is when α is between 1.2~1.3 at a 300mm step length. Fig. 16 shows the deviation of the ZMP and body tilt angle values.

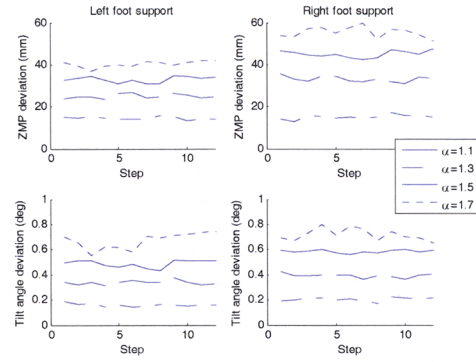


Fig. 13 Deviation of ZMP and θ_p

When α is 1.3~1.4, the deviation of ZMP is approximately 15mm and deviation of θ_p is 0.2 degrees, which is the smallest value.

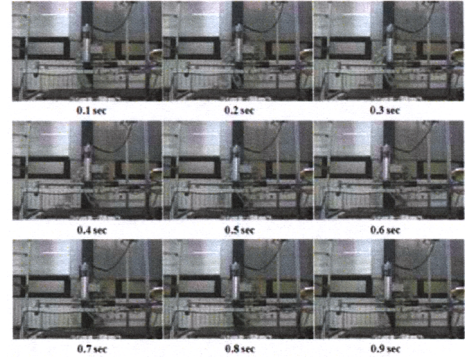


Fig. 14 Walking experiment - 1.8 Km/h

The consumed energy while walking was compared with the walking pattern in a bending knee, and a proposed walking pattern. Fig. 15 shows the used current in walking.

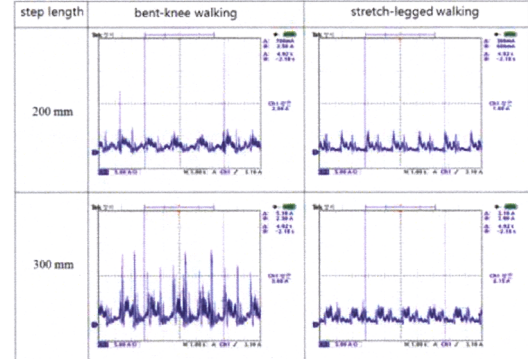


Fig. 15 Comparison of HUBO-walking and proposed walking
TABLE. II
Comparison of Walking Energy

Step length	Bent-knee walking (E1)	Stretch-legged walking(E2)	E2/E1
200 mm	74.0 (J)	61.4 (J)	83 (%)
	2.04 (A)	1.60 (A)	
300 mm	146.9 (J)	83.5 (J)	56 (%)
	3.66 (A)	2.15 (A)	

IV. POSTURE CONTROL

A biped walking robot can be modeled as inverted pendulum. Most inverted pendulum models consider a system to have sufficient stiffness to be considered as a rigid body; however, an actual system has insufficient stiffness. This explains why the stance leg can be deflected caused by a force/torque sensor that is located at the ankle. Hence, it is reasonable to model it as a mass-spring system. Additionally, the swing leg can be oscillated easily because it is a lightly damped system. Fig. 3 shows a robot in the single support phase to consider the deflection of the stance leg and the oscillation of the swing leg.

A. Walking guide platform

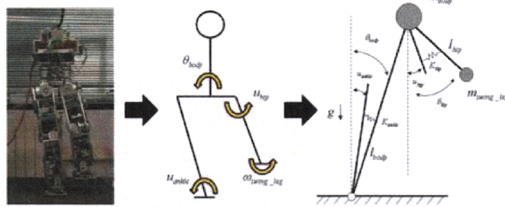


Fig. 16 Modeling of biped robot in single support phase

In Fig. 16 there are two inputs and two outputs. The inputs are u_{ankle} and u_{hip} , u_{ankle} is the reference of the ankle joint of the stance leg and u_{hip} is the reference of hip joint of the swing leg. The outputs are θ_{body} , which denotes the inclination of the body and ω_{swing_leg} which denotes the angular velocity of the swing leg. However, the system can be considered separately because the stiffness of the F/T sensor is much lower than that of the structure and HarmonicDrive, $K_{hip} \gg K_{ankle}$. Thus, the system is decoupled by each of two SISO systems.

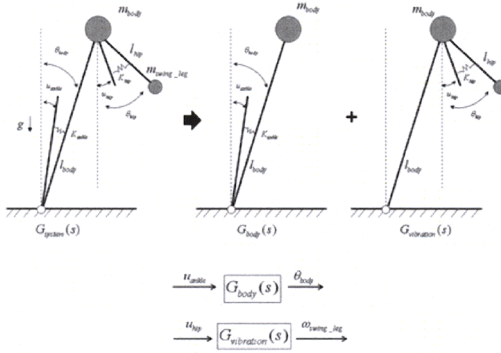


Fig. 17 Decouple of system

In order to judge the stability of a robot in the single support phase, ZMP (Zero Moment Point) [11] is widely used. A robot is considered stable, when the ZMP is located at the supporting polygon. However, as an IMU is used to measure

the posture of a robot, the condition of $\theta_{body} = 0$, $\omega_{swing_leg} \approx 0$ is used in place of ZMP. Moreover the meaning of the ZMP that is located at the supporting polygon is equivalent to $\theta_{body} \approx 0$. Fig. 18 shows a diagram of the control structure. The body balancing controller is designed based on $G_{body}(s)$ and the vibration-reduction controller is designed based on $G_{vibration}(s)$.

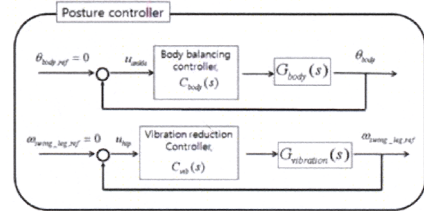


Fig. 18 diagram of posture control

B. Body balancing controller.

Before design a controller, model is acquired by frequency response test.

$$G_{body_roll}(s) = \frac{\theta_{body,roll}}{\theta_{ankle,roll}} = \frac{30.37}{s^2 + 0.9s + 20.25} \quad (7)$$

$$G_{body_pitch}(s) = \frac{\theta_{body,pitch}}{\theta_{ankle,pitch}} = \frac{40.56}{s^2 + 1.04s + 27.04} \quad (8)$$

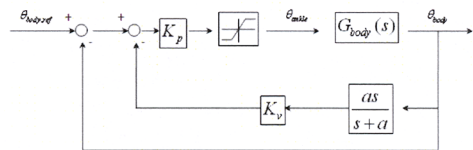


Fig. 19 Block diagram of the body balancing controller

From Eqs. (7) and (8), $G_{body}(s)$ is a lightly damped system with a time constant. The goal is to increase the response and decrease the oscillation. Thus, a body balancing controller composed of a PD-controller and low-pass filter were used.

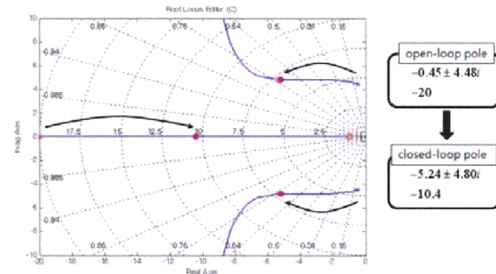


Fig. 20 Root locus of a compensated system

The controller was designed to locate closed-loop poles at $-5.24 \pm 4.8i$, -10.4 with $K_p = 0.2$, $K_v = 1.0$ and, $a = 20$.

C. Vibration-reduction controller.

As with $G_{body}(s)$, $G_{vibration}(s)$ is determined by a frequency response experiment.

$$G_{vibration,pitch}(s) = \frac{\omega_{swing_leg,pitch}}{\theta_{hip,pitch}} = \frac{2500s}{0.09s^3 + 1.45s^2 + 61.25s + 625} \quad (9)$$

$$G_{vibration,roll}(s) = \frac{\omega_{swing_leg,roll}}{\theta_{hip,roll}} = \frac{1366s}{s^2 + 1.48s + 1366} \quad (10)$$

$G_{vibration,pitch}(s)$, $G_{vibration,roll}(s)$ represents a lightly damped system with the damping ratio smaller than 0.1. Thus, a controller was designed to reduce oscillation using a lead-compensator.

$$C_{vib,roll}(s) = 0.04 \frac{0.076s + 1}{0.054s + 1} \quad (11)$$

$$C_{vib,yaw}(s) = 0.158 \frac{0.086s + 1}{0.062s + 1} \quad (12)$$

For the performance test of the designed posture controllers, step response tests were carried out. The ankle joint reference was changed to 1 deg in 2sec. Fig. 21 show the step responses.

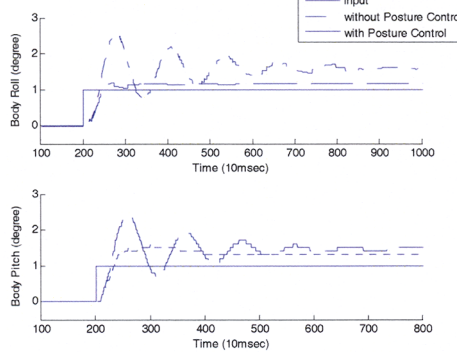


Fig. 21 Comparison of the step response

V. WALKING EXPERIMNT.

A. Walking in place

Walking in place was done at a walking frequency of a 0.8 sec.

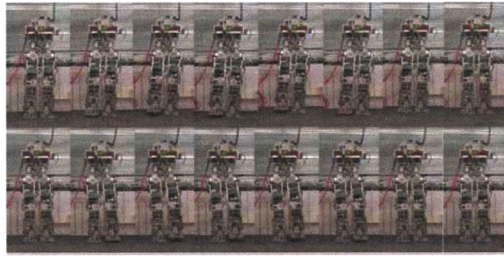


Fig. 22 Sequential photos of walking in place

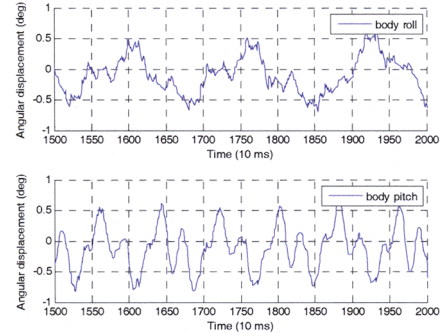


Fig. 23 Plot of the body angle, while walking in place

B. Forward walking

A forward walking experiment was then carried out. The walking speed for this experiment was 1.35 Km/h with a walking frequency of 0.8 sec and a step length of 30 cm.



Fig. 24 Sequential photo of forward walking

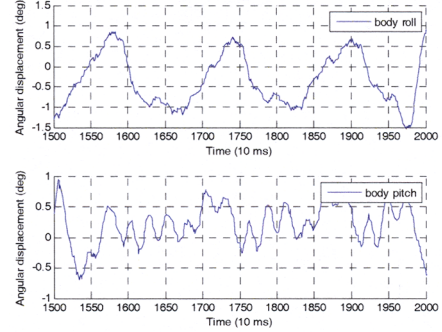


Fig. 25 Plot of the body angle while forward walking

Figs. 23, 25 show the body inclination angle while robot is walking. The body angles were $-0.5^\circ \sim 0.5^\circ$ and $-1.0^\circ \sim 1.0^\circ$ when walking in place and forward walking, respectively. Based on the research of [C. Frigo 8], these values are reasonable. Frigo showed that the standard deviations of the trunk are 1.5° and 2.4° .

VI. CONCLUSION

The proposed walking algorithm using stretch-legged forward walking is thus verified. Additionally, a new system was developed that constrains the motion of a robot in the sagittal plane. It utilizes a treadmill to allow continuous walking in a limited space. As the Walking Guide Platform

(WGP) blocks numerous disturbances, it increases the repeatability of the experiment. After verification of proposed walking pattern, posture control is designed to stabilize robot in single support phase. It maintains posture of body in walking. Stretch-legged walking was realized in humanoid robot through proposed walking pattern and posture control.

ACKNOWLEDGMENT

This research was primarily supported by MOCIE (Ministry of Commerce, Industry and Energy).

REFERENCES

- [1] M. Hirose, Y. Haikawa, T. Takenaka, "The Development of Honda Humanoid Robot," Proc. IEEE Int. Conference on Robotics and Automation, pp. 1321-1326, 1998.
- [2] Kenji KANEKO, Fumio KANEHIRO, Shuji KAJITA, Hirohisa HIRUKAWA, Toshikazu KAWASAKI, Masaru HIRATA, Kazuhiko AKACHI, and Takakatsu ISOZUMI, "Humanoid Robot HRP-2," Proc. IEEE Int. Conference on Robotics and Automation, pp.1083-1090, 2004
- [3] Jung-Yup Kim, Ill-Woo Park, and Jun-Ho Oh, "Design and Walking Control of the Humanoid Robot, KHR-2," International Conference on Control, Automation and Systems, pp. 1539-1543, 2004.
- [4] Ill-Woo Park, Jung-Yup Kim and Jun-Ho Oh, "Online Biped Walking Pattern Generation for Humanoid Robot KHR-3(KAIST Humanoid Robot – 3 : HUBO)," HUMANOIDS 2006, pp 398-403.
- [5] Tad McGeer, "Passive Dynamic Walking," The international journal of robotics research, Vol. 9, No. 2 62-82 ,1990
- [6] Yu Ogura, Hiroyuki Aikawa, Kazushi Shimomura, Hedeki Kondo, akitoshi Morishima, Hun-ok Lim and Atsuo Takanishi, "Human-like Walking with Knee Stretched, Heel-contact and Toe-off Motion by a Humanoid Robot", Proceedings of the 2006 IEEE/RSJ International Conference on Intelligent Robots and Systems, pp 2976-3981.
- [7] E. R. Westervelt, G. Buche, and J. W. Grizzle, "Experimental Validation of a Framework for the Design of Controllers that Induce Stable Walking in Planar Bipeds," *The International Journal of Robotics Research*, Vol. 24, No. 6, June 2004, pp. 559-582.
- [8] C Frigo, R Carabalona, M Dalla Mura, S Negrini, "The upper body segmental movements during walking by young females", *Clinical Biomechanics*, 2003
- [9] S. M. Metev and V. P. Veiko, *Laser Assisted Microtechnology*, 2nd ed., R. M. Osgood, Jr., Ed. Berlin, Germany: Springer-Verlag, 1998.
- [10] J. Breckling, Ed., *The Analysis of Directional Time Series: Applications to Wind Speed and Direction*, ser. Lecture Notes in Statistics. Berlin, Germany: Springer, 1989, vol. 61.
- [11] M. Vukobratovic, B. Boravac, "Zero-moment point – thirty five years of its life", *International Journal of Humanoid Robots*, Vol. 1, No. 1, 2004, pp 157-173